CERN – EUROPEAN ORGANIZATION FOR NUCLEAR RESEARCH

CLIC – Note - 862

ANALYTICAL SOLUTIONS FOR TRANSIENT AND STEADY STATE BEAM LOADING IN ARBITRARY TRAVELING WAVE ACCELERATING STRUCTURES

A. Lunin, V. Yakovlev
Fermilab, P.O.BOX 500, Batavia, IL, USA
A. Grudiev
CERN, CH-1211 Geneva-23, Switzerland

Abstract

Analytical solutions are derived for transient and steady state gradient distributions in the travelling wave accelerating structures with arbitrary variation of parameters over the structure length. The results of both the unloaded and beam loaded cases are presented.

Submitted to the PRST-AB

Geneva, Switzerland
15.12.2010

1. Introduction

The steady state theory of beam loading in electron linear accelerators was developed in 50-th by a number of authors both for constant impedance [1,2,3] and constant gradient [4] accelerating structures. They considered equation for energy conservation in a volume between any two cross sections: the power gain by the beam or power lost in the walls due to Joule effect result in reduction of the power flow. Later on, transient behavior was studied following similar approach, but in this case, in addition to the power dissipated in the walls and gained by the beam, transient change in the energy stored in the volume contributes to the power flow variation along the structure. Again only constant impedance [5,6,7] or constant gradient [8,9] accelerating structures were considered.

On the other hand, traveling wave accelerating structures with arbitrary (neither constant impedance nor constant gradient) geometrical variations over the length are widely used today in order to optimize the structure and linac performance [10,11]. The relationships between structure length, input and average accelerating gradients are obtained numerically solving the energy conservation equation. In this paper, generalized analytical solutions for the steady state and transient gradient distribution in the traveling wave accelerating structure with arbitrary variation of parameters over the structure length are presented. It is based on the method suggested earlier by one of the coauthors [12] and is similar to the classical approach [1-9].

The following definitions are used throughout the paper:

P – Power flow throw the structure cross section

W^* – Stored energy per unit of length

ω – Circular frequency

Q^* – Quality factor

G^* – Loaded accelerating gradient

$\tilde{G}^*$ – Unloaded accelerating gradient

I – Beam current

v_g^* – Group velocity

ρ^* – Normalized shunt impedance, often called R/Q, where R is the shunt impedance per unit of length

z – Longitudinal coordinate

where * denotes that continuous parameters are averaged over the structure period and represent the effective values at individual cell.

The following assumptions are used: a) the structure is perfectly matched at both ends and has no internal reflections, b) all dispersion effects that limit field rise time: $t_r >> c/\omega v_g$, where c is the speed of light, are neglected, c) time of flight of the beam through the structure is much less than the filling time of the structure.

2. Steady State Regime

The basic traveling wave structure relations are:

$$P = W v_g \tag{2.1}$$

$$W = \frac{G^2}{\omega \rho} \tag{2.2}$$

Energy conservation including wall losses and the interaction with the beam gives:

$$\frac{dP}{dz} = -\frac{W\omega}{Q} - GI \tag{2.3}$$

Using Eq. (2.2) in the derivation of the power flow Eq. (2.1) yields:

$$\frac{dP}{dz} = W\frac{dv_g}{dz} + v_g\frac{dW}{dz} = \frac{G^2}{\omega\rho}\frac{dv_g}{dz} + \frac{v_g}{\omega}\left[\frac{2G}{\rho}\frac{dG}{dz} - \frac{G^2}{\rho^2}\frac{d\rho}{dz}\right] \tag{2.4}$$

Substituting Eq. (2.4) to Eq. (2.3) and using Eq. (2.2) results in the first order non-homogeneous differential equation with variable coefficients:

$$\frac{dG}{dz} = -G(z)\alpha(z) - \beta(z) \tag{2.5}$$

where $\alpha(z) = \frac{1}{2}\left[\frac{1}{v_g}\frac{dv_g}{dz} - \frac{1}{\rho}\frac{d\rho}{dz} + \frac{\omega}{v_g Q}\right]$, $\beta(z) = I\frac{\omega\rho}{2v_g}$. The solution of non-homogeneous differential Eq. (2.5) $G(z)$ can be presented as a product of the solution of the homogeneous equation $\widetilde{G}(z)$ and a function $C(z)$:

$$G(z) = \widetilde{G}(z)\cdot C(z) \tag{2.6}$$

where

$$\frac{d\widetilde{G}}{dz} = -\widetilde{G}(z)\alpha(z) \tag{2.7}$$

Substitution Eq. (2.6) to Eq. (2.5) and using Eq. (2.7) yields:

$$\frac{dC(z)}{dz} = -\frac{\beta(z)}{\widetilde{G}(z)} \tag{2.8}$$

Integrating Eq. (2.8) gives:

$$C(z) = -\int_0^z \frac{\beta(z')}{\widetilde{G}(z')}dz' + C_1,$$

where constant $C_1 = 1$ (taking into account the initial condition $G(0) = \widetilde{G}(0)$)

Therefore the general solution of Eq. (2.5) is:

$$G(z) = \widetilde{G}(z)\left[-\int_0^z \frac{\beta(z')}{\widetilde{G}(z')}dz' + 1\right] \tag{2.9}$$

The solution for the homogeneous Eq. (2.7) is:

$$\widetilde{G}(z) = G_0 e^{-\int_0^z \alpha(z')dz'} \tag{2.10}$$

where $G_0 = G(0)$ is a gradient at the beginning of accelerating structure and can be found from initial conditions :

$$G_0 = \sqrt{\frac{\omega\rho(0)P_0}{v_g(0)}} \tag{2.11}$$

where P_0 is input RF power.

The integral of function $\alpha(z)$ can be simplified using analytical solutions:

$$\int_0^z \alpha(z')dz' = \frac{1}{2}\left[\ln\left(\frac{v_g(z)}{v_g(0)}\right) - \ln\left(\frac{\rho(z)}{\rho(0)}\right) + \int_0^z \frac{\omega}{v_g(z')Q(z')}dz'\right] \tag{2.12}$$

Finally we can rewrite Eq. (2.10) as:

$$\widetilde{G}(z) = G_0 \sqrt{\frac{v_g(0)}{v_g(z)}} \sqrt{\frac{\rho(z)}{\rho(0)}} e^{-\frac{1}{2}\int_0^z \frac{\omega}{v_g(z')Q(z')}dz'} = G_0 g(z) \tag{2.13}$$

Eqs. (2.13) and (2.9) give us expression for the loaded gradient:

$$G(z) = \widetilde{G}(z)\left[1 - \int_0^z \frac{I}{\widetilde{G}(z')} \frac{\omega\rho(z')}{2v_g(z')} dz'\right] = G_0 g(z) - g(z)\int_0^z \frac{I}{g(z')} \frac{\omega\rho(z')}{2v_g(z')} dz' \tag{2.14}$$

Table 1: Parameters of the CLIC main linac accelerating structure [10].

	First cell	Middle cell	Last cell
v_g/c [%]	1.65	1.2	0.83
ρ [Ω/m]	14587	16220	17954
Q	5536	5635	5738

The group velocity, normalized shunt impedance and quality factor in the first, middle and last cells of the CLIC main linac accelerating structure are summarized in Table 1 [11]. These parameters have been used to compare accurate solution for arbitrary variation of the structure parameters given by Eq. (2.14) and approximate solution given in [4] for a structure with constant Q-factor and normalized shunt impedance which are taken as for the middle cell but with linear varying group velocity. Both the loaded and unloaded gradients are shown in Fig. 1 for input RF power of 63.1 MW which corresponds to the average loaded gradient of 100 MV/m. In addition, the unloaded gradient has been calculated for 3D model of the structure using Ansoft HFSS [13] frequency-domain finite-element code which takes into account internal reflections. There is clearly a very good agreement between the accurate analytical solution and the numerical simulation. On the contrary, the approximate solution is quite different from the accurate solution mainly due to significant (~30%) variation of the shunt impedance along the structure, see Table 1.

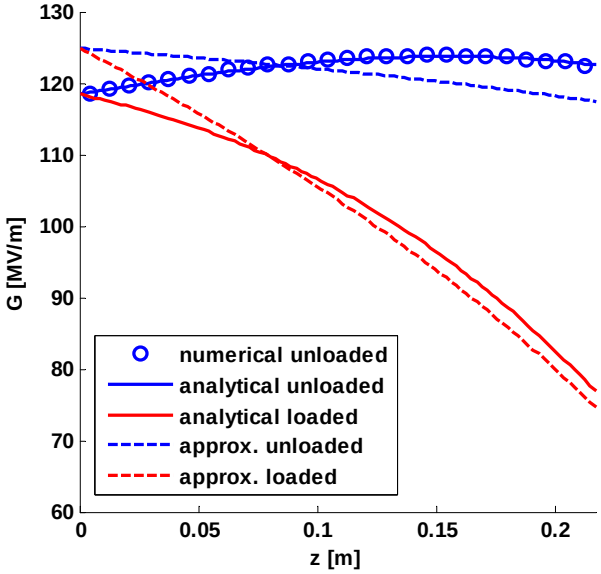

Fig. 1 Loaded (red) and unloaded (blue) gradients calculated accurately (solid) and approximately (dashed) for CLIC main linac accelerating structure. In blue circles, the unloaded gradient calculated numerically is shown.

3. Transient Regime

The transient regime can also be derived analytically. The instantaneous energy conservation is given by:

$$\frac{\partial W}{\partial t} = -\frac{dP}{dz} - \frac{W\omega}{Q} - GI \tag{3.1}$$

Substituting Eqs. (2.1), (2.2) and (2.4) into Eq. (3.1) yields:

$$\frac{\partial G}{\partial t} = -\frac{G}{2}\frac{dv_g}{dz} - v_g\frac{dG}{dz} + \frac{v_g G}{2\rho}\frac{d\rho}{dz} - \frac{\omega G}{2Q} - \frac{\omega\rho}{2}I \tag{3.2}$$

We assume the following initial conditions:

$$\begin{aligned} &G(0,t) = G_0(t), \quad \text{at } z = 0 \\ &G(z,0) = 0, \qquad \text{at } t = 0 \end{aligned} \tag{3.3}$$

Using Laplace transformation of a function $G(t)$: $\hat{G}(p) = L\{G(t)\} = \int_0^\infty e^{-pt}G(t)dt, \quad t \ge 0$, its differentiation property: $L\left\{\frac{dG}{dt}\right\} = p\hat{G} - G(z,0)$ and taking into account Eqs. (3.3) we can write Eq. (3.2) after Laplace transformation:

$$p\hat{G} = -\frac{\hat{G}}{2}\frac{dv_g}{dz} - v_g\frac{d\hat{G}}{dz} + \frac{v_g\hat{G}}{2\rho}\frac{d\rho}{dz} - \frac{\omega\hat{G}}{2Q} - \frac{\omega\rho}{2}\hat{I} \tag{3.4}$$

First, we consider unloaded case ($I = 0$). Then Eq. (3.4) becomes homogeneous differential equation:

$$\frac{d\hat{\tilde{G}}}{dz} = -\hat{\tilde{G}}(z,p)\hat{\alpha}(z,p) \tag{3.5}$$

where $\hat{\alpha}(z,p) = \frac{1}{2}\left[\frac{1}{v_g}\frac{dv_g}{dz} - \frac{1}{\rho}\frac{d\rho}{dz} + \frac{\omega}{v_g Q} + \frac{2p}{v_g}\right]$. The solution of Eq. (3.5) is obtained similar to that of the Eq. (2.7) as:

$$\hat{\tilde{G}}(z,p) = \hat{\tilde{G}}(0,p)e^{-\int_0^z \hat{\alpha}(z',p)dz'} = \hat{\tilde{G}}(0,p)g(z)e^{-p\int_0^z \frac{dz'}{v_g(z')}} \tag{3.7}$$

where $g(z)$ is defined in Eq. (2.13). The time-domain solution of Eq. (3.7) is obtained by applying inverse Laplace transformation and its time shifting property: $L^{-1}\{F(p)e^{-p\tau}\} = f(t-\tau)H(t-\tau)$, where $H(t-\tau)$ is the Heaviside step function and

$$\tau(z) = \int_0^z \frac{dz'}{v_g(z')} \tag{3.8}$$

is the signal time delay. Thus, the distribution of the unloaded gradient in time-domain along the structure is:

$$\tilde{G}(z,t) = G_0[t - \tau(z)]g(z)H[t - \tau(z)] \tag{3.9}$$

or taking into account Eqs. (2.11) and (2.13) it can be expressed as a function of the input RF power:

$$\tilde{G}(z,t) = \sqrt{P_0[t-\tau(z)]}\sqrt{\frac{\omega\rho(z)}{v_g(z)}}e^{-\frac{1}{2}\int_0^z \frac{\omega}{v_g(z')Q(z')}dz'} H[t-\tau(z)] \tag{3.10}$$

The solution of non-homogeneous Eq. (3.4) is obtained similar to the solution of Eq. (2.5) as product of solution of homogeneous equation $\hat{\tilde{G}}(z,p)$ and a function $\hat{C}(z,p)$:

$$\hat{G}(z,p) = \hat{\tilde{G}}(z,p)\cdot\hat{C}(z,p) \tag{3.11}$$

Then Eq. (3.4) becomes

$$\frac{d\hat{G}}{dz} = \frac{d\hat{\tilde{G}}}{dz}\hat{C} + \frac{d\hat{C}}{dz}\hat{\tilde{G}} = -\hat{G}(z,p)\hat{\alpha}(z,p) - \hat{\beta}(z,p) \tag{3.12}$$

where $\hat{\beta}(z,p) = \hat{I}\frac{\omega\rho}{2v_g}$.

Substituting Eqs. (3.5) and (3.11) into Eq. (3.12) yields:

$$\hat{\tilde{G}}\frac{d\hat{C}}{dz} = -\hat{\beta}(z,p) \tag{3.13}$$

and furthermore using Eqs. (3.7) and (3.8)

$$\hat{\tilde{G}}(0,p)g(z)e^{-p\tau(z)}\frac{d\hat{C}}{dz} = -\hat{\beta}(z,p) \tag{3.14}$$

Solution of Eq. (3.14) can be obtained by integration in the form:

$$\hat{\tilde{G}}(0,p)\hat{C}(z,p) = -\int_0^z \frac{\hat{\beta}(z',p)}{g(z')}e^{p\tau(z')}dz' + \hat{C}_1(p) \tag{3.15}$$

where $\hat{C}_1(p) = \hat{\tilde{G}}(0,p)$ (taking into account initial condition $\hat{G}(0,p) = \hat{\tilde{G}}(0,p)$). Note, that $g(z) > 0$. Finally, the general solution of Eq. (3.4) is derived using Eqs. (3.7, 3.11 and 3.15):

$$\begin{aligned}\hat{G}(z,p) &= \hat{\tilde{G}}(0,p)\hat{C}(z,p)g(z)e^{-p\tau(z)} \\ &= \left[\hat{\tilde{G}}(0,p) - \int_0^z \frac{\hat{\beta}(z',p)}{g(z')}e^{p\tau(z')}dz'\right]g(z)e^{-p\tau(z)} \\ &= \hat{\tilde{G}}(z,p) - g(z)\int_0^z \frac{\hat{\beta}(z',p)}{g(z')}e^{-p[\tau(z)-\tau(z')]}dz'\end{aligned} \tag{3.16}$$

Thus the time-dependent solution of Eq. (3.1) is obtained by applying inverse Laplace transform to Eq. (3.16). Here again the time shifting property has been used:

$$\begin{aligned}G(z,t) &= G_0[t-\tau(z)]g(z)H[t-\tau(z)] \\ &- g(z)\int_0^z \frac{I[t-\tau(z)+\tau(z')]H[t-\tau(z)+\tau(z')]}{g(z')}\frac{\omega\rho(z')}{2v_g(z')}dz'\end{aligned} \tag{3.17}$$

where, $\tau(z)$ is the function of coordinate given by Eq. (3.8).

The first term on the right hand side of Eq. (3.17) is the solution of the homogeneous equation for the unloaded gradient obtained above Eq. (3.9) or Eq. (3.10) in terms of the input power. The second term is the so-called beam induced gradient which is the difference between the loaded and unloaded gradient distributions.

The time-dependent solution given by Eq. (3.17) during the transient related to structure filling and to beam injection is illustrated in Fig. 2 (a) and (b), respectively, for the CLIC main linac accelerating structure with the parameters from the Table 1. In Fig. 3, the corresponding input power and beam current time dependences are shown together with the unloaded, loaded and beam voltages defined as:

$$V(t)=\int_0^L G(z,t)\,dz\,,\qquad \tilde{V}(t)=\int_0^L \tilde{G}(z,t)\,dz\,,\qquad V_b(t)=V(t)-\tilde{V}(t)$$

respectively, where L is the structure length. The rise time t_r is 21 ns $>> c/\omega v_g$, the beam time t_b is 156 ns and the beam current $I=eN_e f_b=1.6\times10^{-19}\cdot3.72\times10^{9}\cdot2\times10^{9}$ is 1.2 A [10]. The structure filling time $t_f=\tau(L)$ is 66.7 ns.

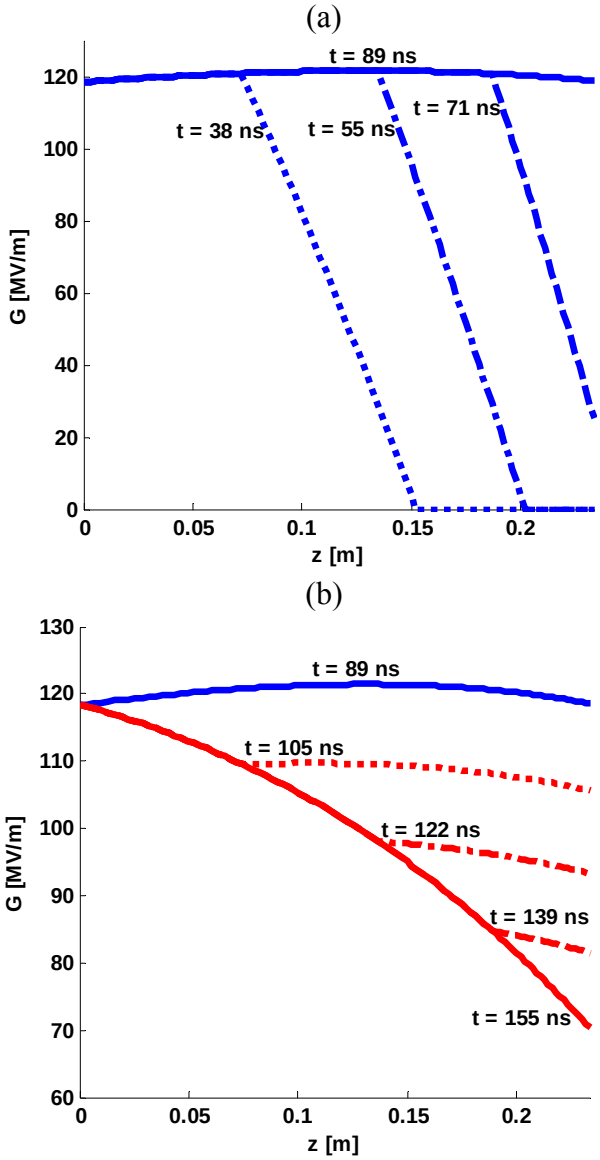

Fig. 2 The instantaneous unloaded (blue) and loaded (red) gradient distributions along the structure at different moments of time during the transient related to structure filling (a) and to the beam injection (b). The steady state solutions are shown as well (solid lines).

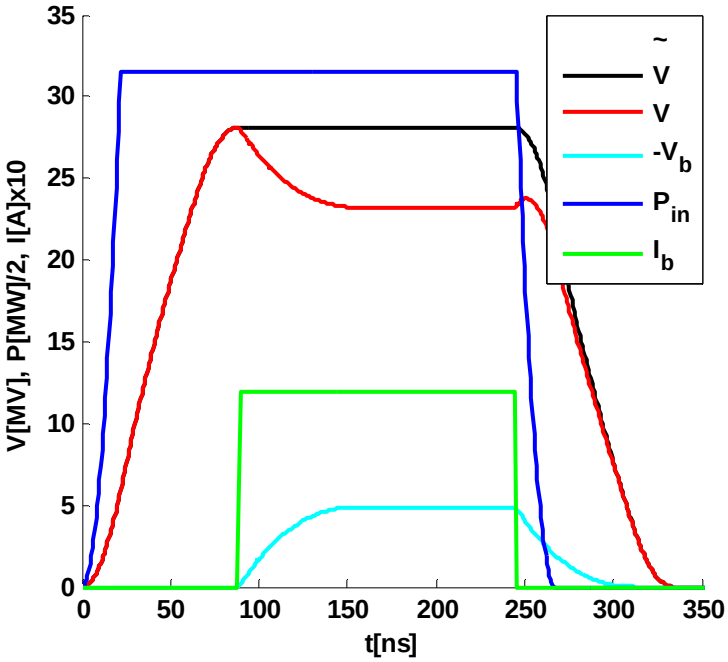

Fig. 3 The time dependence of the input RF power (blue) with the rise time of 21 ns, beam current (green) and the corresponding unloaded (black), loaded (red) and beam (light blue) voltages are shown.

The change in the loaded voltage right after injection due to the transient beam loading of the structure causes energy spread along the beam. One of the possible methods of compensation of this transient beam loading effect is presented in the next section.

4. Compensation of the transient beam loading

The idea of the transient beam loading compensation is similar to the one used in [14] where linear ramp of the input RF amplitude has been applied to compensate the bunch-to-bunch energy variation to first order. In this paper, exact modification of the input power during a feeling time t_f is calculated in order to bring the gradient distribution at injection equal to the steady-state loaded gradient solution $G(z)$. Based on Eq. (3.9) the instantaneous gradient distribution at the moment of injection $t = t_f$ is:

$$G(z,t_f) = \tilde{G}(z,t_f) = G_0[t_f - \tau(z)]g(z) \qquad (4.1)$$

At the same time, the steady state beam loaded solution is expressed by (2.14). Equating Eq. (4.1) and Eq. (2.14) the required time dependence for the input gradient $G_0(t)$ during the feeling time is obtained:

$$G_0[t_f - \tau(z)]g(z) = G_0(t_f)g(z) - g(z)\int_0^z \frac{I}{g(z')}\frac{\omega\rho(z')}{2v_g(z')}dz' \qquad (4.2)$$

where $G_0(t_f)$ is the steady-state value of the input gradient after injection. The input gradient in Eq. (4.2) indirectly depends on time. Introducing function $z(t)$ as a solution of the following integral equation:

$$t(z) = \int_{z}^{L} \frac{dz'}{v_g(z')} \tag{4.3}$$

Eq. (4.2) becomes an explicit function of time:

$$G_0(t) = G_0(t_f) - \int_{0}^{z(t)} \frac{I}{g(z')} \frac{\omega\rho(z')}{2v_g(z')} dz' \tag{4.4}$$

Expression for the input RF power is derived using Eq. (2.11):

$$P_0(t) = P_0(t_f)\left[1 - \sqrt{\frac{v_g(0)}{\omega\rho(0)P_0(t_f)}} \int_{0}^{z(t)} \frac{I}{g(z')} \frac{\omega\rho(z')}{2v_g(z')} dz'\right]^2 \tag{4.5}$$

where $P_0(t_f)$ is the steady-state value of the input RF power after injection. The solution of Eq. (4.5) is shown in Fig. 4 (blue) together with the beam current (green) injected exactly at the end of the ramp and the corresponding unloaded (black), loaded (red) and beam (light blue) voltages. The loaded voltage is flat during the time when the beam is present in the structure and the transient related to the beam injection is fully compensated, at least in the framework of this analytical model (see introduction for the assumptions made). The gradient distribution at different moments of time is presented for the compensated case in Fig. 5 (a) and (b) for the structure filling transient and the beam injection transient, respectively.

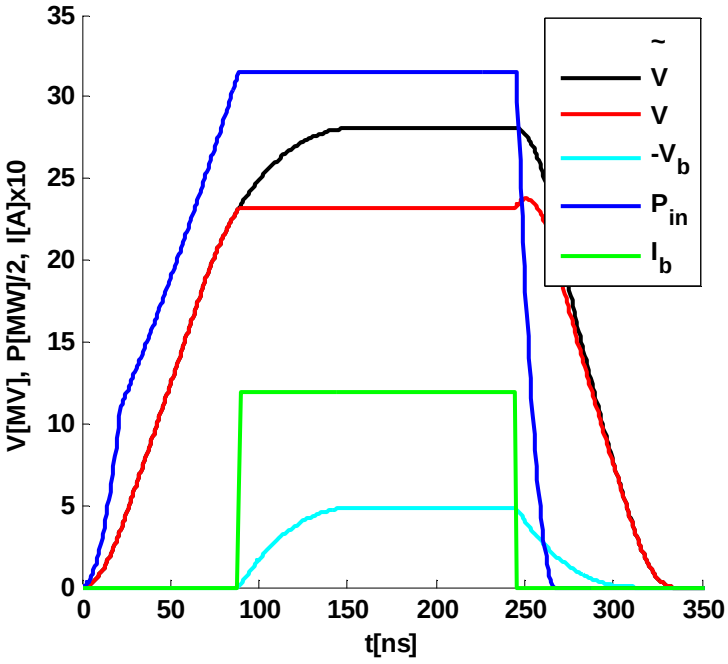

Fig. 4 The input RF pulse profile with 21 ns rise time and ramp-up during the feeling time for the transient beam loading compensation is shown in blue. Beam current injected exactly at the end of the ramp is shown in green. The corresponding unloaded, loaded and beam voltages are shown in black, red and light blue, respectively.

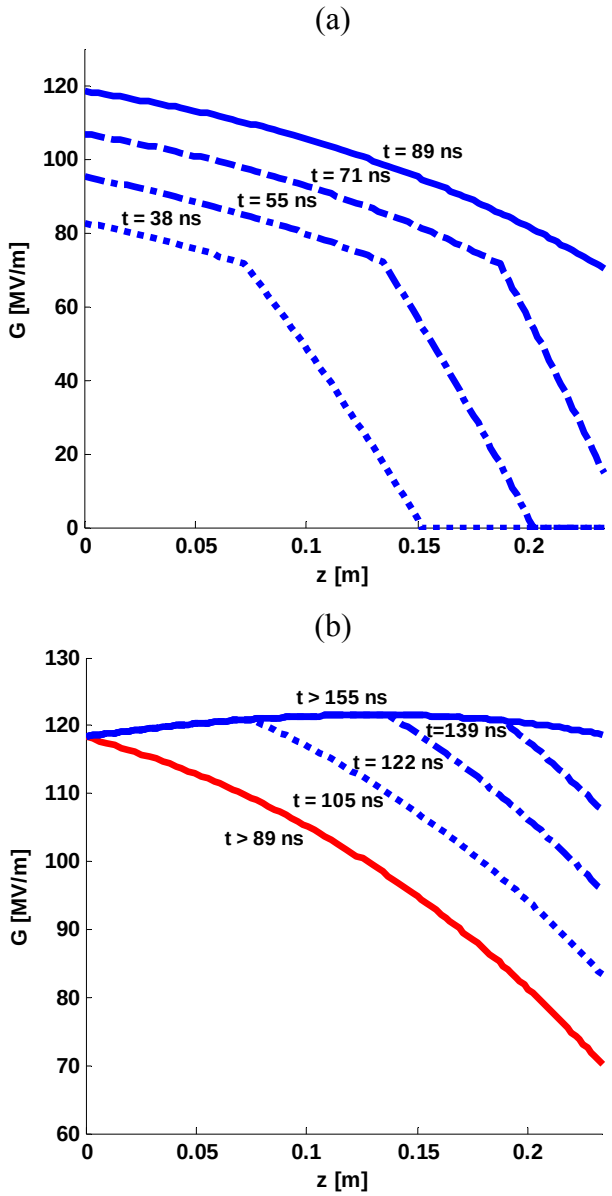

Fig. 5 The instantaneous unloaded gradient distribution along the structure at different moments of time during the structure filling is presented in (a). Special correction to the input RF pulse was applied (see Fig.4). In (b), the instantaneous unloaded gradient at different time moments after beam injection is shown in blue. Solid lines represent the steady state distributions for loaded (red) and unloaded (blue) gradients. Beam injection time is 89 ns.

Summary

Analytical expressions for unloaded and loaded gradient distributions in travelling wave structures with arbitrary variation of parameters were derived in steady state and in transient. They were applied to the case of the CLIC main linac accelerating structure. The obtained analytical solution agrees very well with the numerical solution obtained using finite-element code. On the other hand, it differs from the approximate solution obtained using expressions derived earlier in [4].

Acknowledgements
The authors are thankful to W. Wuensch for careful reading the manuscript.

References
1. K. Johnsen, Heavy Beam Loading in Linear Electron Accelerators, Proc. Phys. Soc. VB 64 (1951) 1062.
2. G. Saxon, Theory of Electron Beam Loading in Linear Accelerators, Proc. Phys. Soc. VB 67 (1954) 705.
3. R. B. Neal, Design of Linear Electron Accelerators with Beam Loading, J. Appl. Phys. 29, (1958), 1019; or M. L. Report no. 379, W. W. Hansen Laboratories, Stanford (1957).
4. R. B. Neal, Theory of the Constant Gradient Linear Electron Accelerator, M. L. Report no. 513, W. W. Hansen Laboratories, Stanford (1958).
5. R. B. Neal, Transient Beam Loading in Linear Electron Accelerators, M. L. Report no. 388. (1957).
6. J. E. Leiss, Transient Beam Loading in Linear electron Accelerators, NBS Internal Report (September 1958).
7. J. E. Leiss, Beam Loading and Transient Behavior in Travelling Wave Electron Linear Accelerators, In Linear Accelerators, ed., A. Septier and P.M. Lapostolle. Amsterdam: North-Holland Publishing Company, 1969,
8. L. Burnod, Regime transitoire dans les accelerateurs lineaires, LAL Report no. 17, Orsay (1961).
9. J. W. Wang, RF Property of Periodic Accelerating Structures for Linear Colliders, Ph.D. Dissertation, SLAC-339, (1989).
10. R. H. Miller et al., A Damped Detuned Structure for the Next Linear Collider, Proc. Linac96, Geneva (1996).
11. A. Grudiev, W. Wuensch, Design of the CLIC main linac accelerating structure for CLIC Conceptual design report, Proc. LINAC10, Tsukuba (2010).
12. M.M. Karliner, O.A. Nezhevenko, B.M. Fomel, V.P. Yakovlev, "On Comparison of Accelerating Structures, Operating in the Stored Energy Mode", Preprint INP 86-146, Novosibirsk, 1986, (in Russian).
13. Ansoft HFSS, www.ansoft.com.
14. K. A. Thompson, R. D. Ruth, Simulation and Compensation of Multibunch Energy Variation in NLC, Proc. PAC93, Washington, D.C. (1993).